Cell, Vol. 83, 503–512, November 3, 1995, Copyright © 1995 by Cell Press

Acetylcholinesterase Inhibition by Fasciculin: Crystal Structure of the Complex

Yves Bourne,*† Palmer Taylor,* and Pascale Marchot*
*Department of Pharmacology
University of California, San Diego
La Jolla, California 92093-0636
†Department of Molecular Biology
The Scripps Research Institute
La Jolla, California 92037

Summary

The crystal structure of the snake toxin fasciculin, bound to mouse acetylcholinesterase (mAChE), at 3.2 Å resolution reveals a synergistic three-point anchorage consistent with the picomolar dissociation constant of the complex. Loop II of fasciculin contains a cluster of hydrophobic residues that interact with the peripheral anionic site of the enzyme and sterically occlude substrate access to the catalytic site. Loop I fits in a crevice near the lip of the gorge to maximize the surface area of contact of loop II at the gorge entry. The fasciculin core surrounds a protruding loop on the enzyme surface and stabilizes the whole assembly. Upon binding of fasciculin, subtle structural rearrangements of AChE occur that could explain the observed residual catalytic activity of the fasciculin-enzyme complex.

Introduction

Acetylcholinesterase (AChE), which terminates the action of the neurotransmitter acetylcholine (ACh) at cholinergic synapses in the central and peripheral nervous systems, is a target site for a variety of pharmacologic agents, insecticides in widespread use, and nerve gases (Massoulié et al., 1993; Taylor and Radić, 1994). The Torpedo californica AChE (TcAChE) molecule, with its α/β hydrolase fold (Sussman et al., 1991), has defined the structures of a large family of enzymes that includes other esterases and several lipases, as well as proteins without hydrolase activity (Cygler et al., 1993). The active center triad, consisting of the catalytic Ser-200, Glu-327, and His-440 in TcAChE, is found nearly centrosymmetric to the subunit at the bottom of a narrow gorge. The narrow gorge width, coupled with its depth of 18–20 Å, has raised questions regarding the compatibility of these dimensions with a near diffusion-limited rate of substrate entry and catalysis (Tan et al., 1993). The charge distribution on the enzyme creates a dipole that not only directs ligands to the gorge entry, but may also facilitate diffusion to the active center. This, in turn, has led to the suggestion of a "back door," a portal of substrate access distinct from the gorge entrance, to accommodate the rapid product removal or solvent contact (Ripoll et al., 1993; Gilson et al., 1994). However, mutations of AChE in areas where solvent exposure to the gorge might be increased have not yielded evidence for a second site of access (Shafferman et al., 1994). Inhibitors, in addition to binding at the active center, may associate with a peripheral anionic site, remote from the active center, to influence catalysis allosterically. Labeling and site-specific mutagenesis studies indicate that this site resides near the lip of the active center gorge (for review see Taylor and Radić, 1994).

Fasciculins are 61 amino acid peptides isolated from mamba (Dendroaspis) venoms. They belong to the family of three-fingered snake toxins that includes the α-neurotoxins, selective nicotinic receptor blockers (Changeux et al., 1970; Endo and Tamiya, 1991), and the subtype-specific muscarinic receptor agonists (Adem et al., 1988; Segalas et al., 1995). The fasciculins are the only known peptidic AChE inhibitors and are highly selective; they inhibit mammalian and electric eel AChE with K_i values in the picomolar range, but have only micro- to millimolar K_is for avian and insect AChEs and for butyrylcholinesterases (BuChE) (for review see Cerveñansky et al., 1991). Chemical labeling (Duran et al., 1994), ligand competition (Karlsson et al., 1984; Marchot et al., 1993; Radić et al., 1995; Eastman et al., 1995), and site-directed mutagenesis studies (Radić et al., 1994, 1995), indicate that fasciculin does not completely occlude ligand access to the active center Ser, but rather binds to the peripheral site to inhibit catalysis, perhaps allosterically. Although the X-ray structures of the fasciculins Fas1 and Fas2 have been solved (Le Du et al., 1992; 1995), they have not revealed the nature of the binding interface.

To delineate the structural determinants of the fasciculin specificity for AChE and how the fasciculins inhibit AChE, we have determined the crystal structure of the complex formed between Fas2 and a recombinant monomeric AChE from mouse (mAChE) and refined it to 3.2 Å resolution. The current model (model A) contains one molecule of mAChE (residues 4–257 and 265–543; Rachinsky et al., 1990), one molecule of Fas2 (residues 1–61), and one N-acetylglucosamine (GlcNAc) moiety linked to mAChE at Asn-350. The structure, which has an excellent stereochemistry with a R factor of 18.4% for data between 10 and 3.2 Å, reveals the nature of AChE inhibition by Fas2 with implications for the binding of structurally related α-neurotoxins and muscarinic agonists to their respective ACh receptors.

Results and Discussion

Overall Structure of the Complex

The excellent quality of the 3.2 Å electron density map unambiguously reveals the positions of the side chains in Fas2 and mAChE, as well as those located at the interface of the complex (Figure 1). The mAChE molecule has the α/β hydrolase fold and consists of the same 12-stranded central-mixed β sheet surrounded by 14 α helices as the TcAChE molecule (Sussman et al., 1991). Secondary structure motifs are specified according to Cygler et al. (1993): the strands of the small amino-terminal β sheet

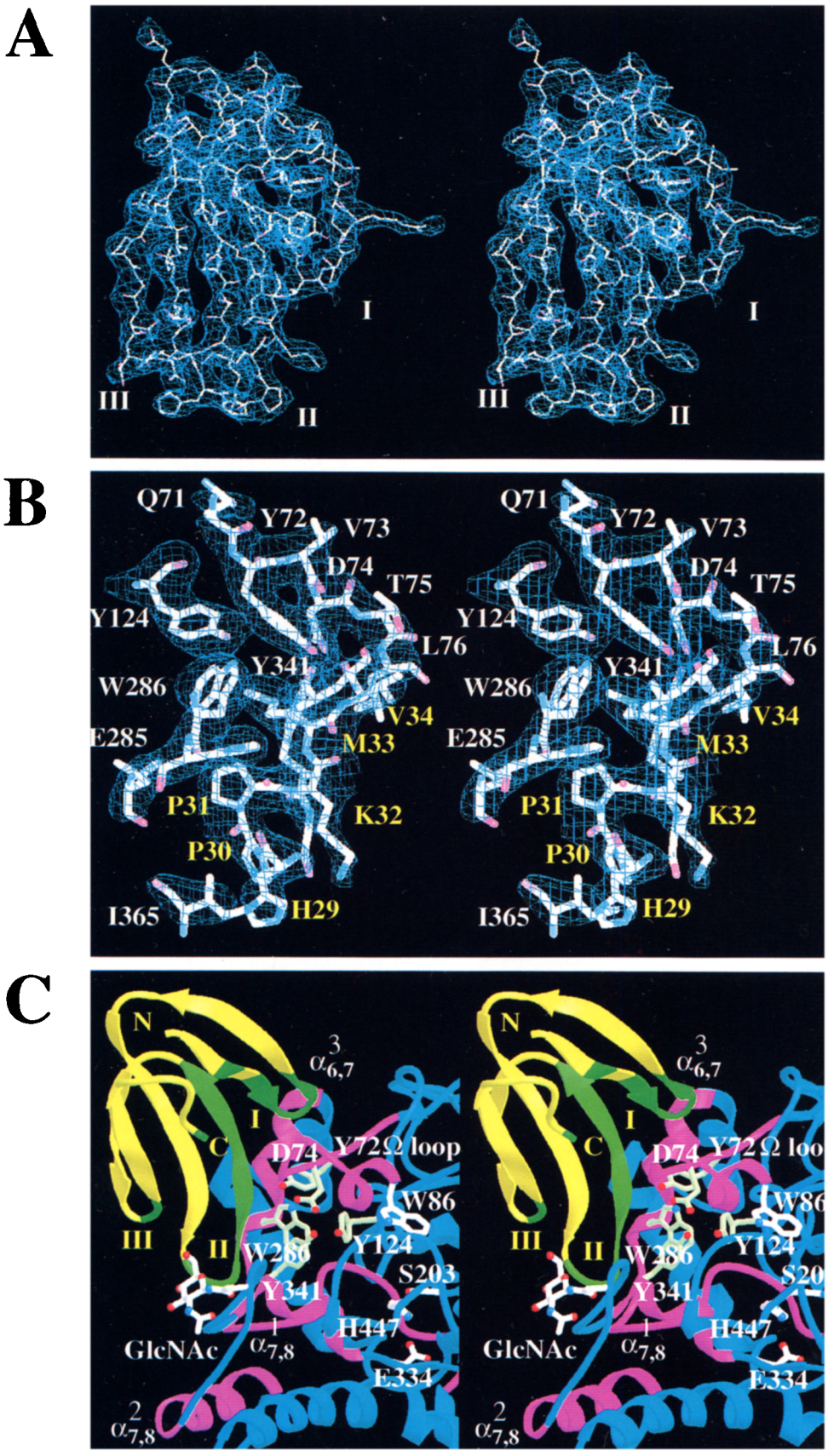

Figure 1. Quality of the Structure and Overall View of the Complex

(A) Stereoview of the final σ_A weighting $2F_o - F_c$ electron density map (contoured at 1 σ) of the entire Fas2 molecule at 3.2 Å resolution. Labels I, II, and III refer to Fas2 loop I (residues 4–16), loop II (residues 23–38), and loop III (residues 42–51). The Fas2 molecule is particularly well ordered in the complex. The Arg-11 side chain extends on the right of the molecule.

(B) Stereoview of the 3.2 Å resolution omit $F_o - F_c$ electron density map of the tip of Fas2 loop II and the surrounding mAChE residues (5% of the total number of atoms, contoured at 2.5 σ). The coordinates of this region were omitted and the protein coordinates refined by simulated annealing before the phase calculation for the map. Residues are labeled in white for mAChE and in yellow for Fas2.

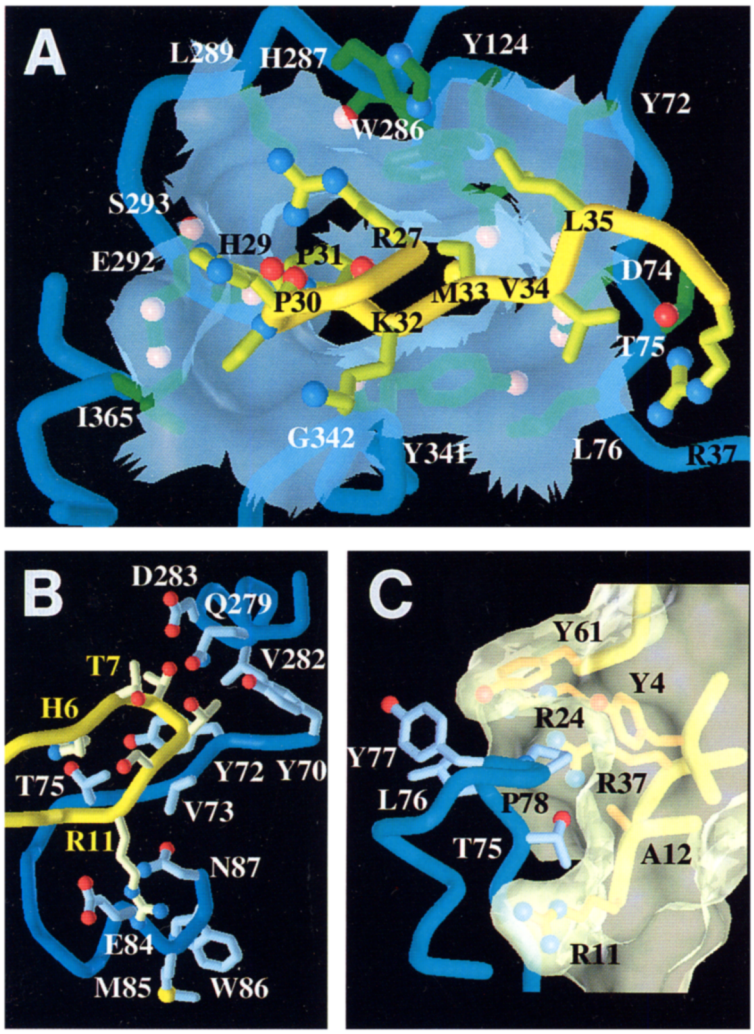

Figure 2. Three-Point Interface of the Fas2–mAChE Complex

(A) Side chain to side chain interactions between mAChE (blue Cα tubes with green side chains and colored spheres) and the tip of Fas2 loop II (yellow Cα tubes with light yellow side chains and colored sphere). A part of the molecular surface of mAChE buried in the complex is displayed in transparency and shows the cavities around the gorge entrance for Fas2 Pro-30, Pro-31, and Met-33. The tip of Fas2 loop II interacts with mAChE peripheral anionic site residues Tyr-72(70), Tyr-124(121), Trp-286(279), Tyr-341(334), and Gly-342(335). Extensive polar and van der Waals interactions between Fas2 loop II and mAChE residues surrounding the gorge entrance stabilize this interface of the complex.

(B) Side chain to side chain interactions between mAChE (blue Cα tubes with light blue side chains and colored spheres) and the tip of Fas2 loop I (yellow Cα tubes with light yellow side chains and colored spheres). The side chain of Fas2 Arg-11 comes in close apposition with mAChE Glu-84(82) and Asn-87(85) and surrounds mAChE Trp-86(84), a proposed second portal for entry of substrate and exit of product (Gilson et al., 1994). mAChE Asp-283(276) and Gln-279(272), suspended from helix $\alpha^3_{6,7}$, are hydrogen bonded to Fas2 Thr-8 and Thr-9. For clarity, Fas2 residues Thr-8, Thr-9, and Ser-10 at the tip of loop I are not labeled, but their side chains are clearly visible. The capacity for hydrogen bonding of the hydroxyl groups of Thr-8 and Thr-9 is evident.

(C) Side chain to side chain interactions between mAChE (blue Cα tubes with light blue side chains and colored spheres) and the core region of Fas2 (yellow Cα tubes with orange side chains and colored spheres). The cavity formed at the molecular surface of Fas2 by the side chains of Arg-11 (protruding at the front), Ala-12, Tyr-4, and Tyr-61 is filled by mAChE Pro-78(76). Fas2 Arg-24, a structurally important residue, is hydrogen bonded to the carbonyl atom of Tyr-61 and stabilizes the carboxy-terminal region of Fas2. Fas2 Arg-37, a residue conserved in the three-fingered peptide toxin family, is in stacking interaction with Fas2 Arg-24 and is hydrogen bonded to mAChE Thr-75(73).

are identified as β_i; the strands of the large central β sheet are identified as β_j; the α helices are identified as $\alpha^k_{i,j}$, where subscripts refer to the loop-connecting strands i and j of the β sheet in which the helix is embedded, and superscripts refer to the sequential number of this helix within the loop (no superscript is used when there is a single helix in the connecting loop). The number in parentheses that follows the mAChE residue number denotes the corresponding position in the TcAChE sequence.

The Fas2 molecule consists of two antiparallel β sheets with a three-stranded β sheet formed by residues 22–27, 34–39, and 48–53 and a short two-stranded β sheet formed by residues 3–4 and 14–15 (Le Du et al., 1992). Fas2, with its three loops emerging from a dense core containing the disulfide bridges, forms a slightly concave flat disk that fits into an elongated cavity at the surface of mAChE (Figure 1C). This cavity, located between helix $\alpha^3_{6,7}$ and the Ω loop Cys-69(67) to Cys-96(94), which corresponds to the lid region in lipases (Grochulski et al., 1994), forms the entrance of the mAChE active site gorge. The inner side of Fas2 β strand 4 is oriented roughly 45° away from the direction of the gorge entrance. Three distinct, separated anchorage points of Fas2 on mAChE result in a particularly well-ordered molecule of bound Fas2 (Figures 1 and 2) consistent with its picomolar dissociation constant for mAChE. All three regions of Fas2 responsible for com-

(C) Stereoview ribbon diagram of Fas2 (yellow and green) bound to mAChE (blue and magenta). The tip of loop II and the inner side of β strand 4 of Fas2 are tightly associated with the peripheral anionic site of mAChE, whereas loop I binds on the other side of the lid region (Ω loop) of mAChE. The residues of Fas2 and the secondary structure elements of mAChE involved in the complex are highlighted in green and in magenta, respectively. Residues within the mAChE catalytic site, Ser-203(200), Glu-334(327), His-447(440), and Trp-86(84), are displayed as white bonds with colored spheres. Residues belonging to the mAChE peripheral anionic site, Tyr-72(70), Asp-74(72), Trp-286(279), and Tyr-341(334), are displayed as green bonds with colored spheres. The GlcNAc moiety linked to Asn-350(343) is displayed in white with colored spheres. Secondary structure elements of mAChE are labeled according to Cygler et al. (1993).

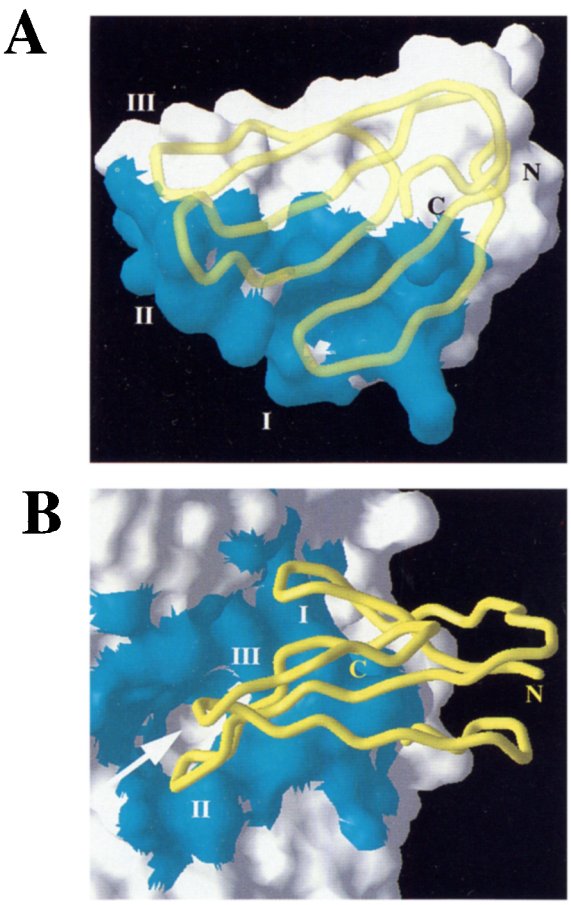

Figure 3. Molecular Surfaces of Fas2 and mAChE at the Complex Interface

(A) Fas2 molecular surface, colored in blue for the residues buried to a 1.6 Å probe radius and shown in white for the nonburied residues. A Cα trace (yellow) is shown through the surface. The buried residues are found at the tip of loop I (bottom center), where Arg-11 is clearly visible (bottom) and at the tip of loop II (middle left) and extend to the concave face of β strand 4 (center). Only two residues are buried at the tip of loop III (back left). This interfacial area represents 27% of the total accessible surface area of Fas2 and comprises 21 residues of Fas2, of which only four are positively charged. The cavity formed by the side chains of Tyr-4, Arg-37, and Tyr-61 is visible at the center of the molecule.

(B) mAChE molecular surface, viewed looking down into the gorge. The color code is the same as in (A). Buried residues cluster in and largely around the gorge of the enzyme and on the other side of the lid region (top). This interface area represents 5% of the total accessible surface area of the molecule and comprises 25 residues of mAChE. Fas2 (yellow Cα trace) is superimposed on the molecular surface and is oriented ~90° away from that in (A). Labels I, II, and III refer to the loops of Fas2. The arrow indicates the active site gorge entrance.

plex formation are located in the concave face of the molecule (Figures 1C and 3A).

Detailed Structure of the Complex

Loop II of Fas2, formed by residues Tyr-23 to Arg-38, is central to the interface (Figure 1C). The tip of loop II, which contains the Pro–Pro–Lys–Met sequence motif characteristic of the fasciculin family, is tightly bound to the peripheral anionic site along with numerous residues surrounding the gorge entrance in mAChE (including residues from the lid and from helices $\alpha^3_{6,7}$, $\alpha^1_{7,8}$, and $\alpha^2_{7,8}$) and sterically occludes substrate access to the gorge (Figures 1C, 2A, and 3B). Loop II residue Met-33 establishes several key van der Waals contacts with mAChE Tyr-72(70), Tyr-124(121), and Tyr-341(334) and packs against mAChE Trp-286(279) (Figure 2A). Predominant hydrophobic interactions are found between Fas2 Pro-30 and Pro-31 and mAChE Ile-365(358) and Leu-289(282), which form a tight cluster of buried residues at the binding interface. The side chains of Fas2 His-29 and Pro-30 also participate in van der Waals interactions with the side chain of mAChE Glu-292 (Asp-285 in TcAChE), one of the few acidic residues present at the top of the gorge and contributing to its negative charge (Sussman et al., 1991). In addition, Fas2 Val-34 and Leu-35 in β strand 4 establish van der Waals contacts with mAChE Leu-76(74), Tyr-72(70), and His-287(280). The unusual shape of loop II, comprised of two vicinal Pro residues at its tip with Pro-30 in the *cis* conformation, fits perfectly the mAChE peripheral anionic site without requiring a dramatic conformational change in the two partners of the complex (Figures 1C, 2A, 3B, and 4A). In addition, Fas2 Arg-27 is hydrogen bonded to Fas2 His-29, Pro-30, and Pro-31 and to mAChE Trp-286(279) carbonyl oxygen atoms and thus stabilizes the conformation of the entire loop in bound Fas2 (Figure 2A). Polar interactions are established between the nitrogen atom of Fas2 Pro-31 and the carbonyl oxygen atom of mAChE Ser-293(286), between the amide backbone nitrogen of Fas2 Lys-32 and the carbonyl oxygen atom of mAChE Tyr-341(334), and between the side chains of Fas2 Arg-37 and mAChE Thr-75(73). A critical role is played by mAChE Gly-342(335), which is in van der Waals contact with the side chain of Fas2 Lys-32 and, thus, cannot be substituted by a larger side chain without perturbing the complex.

The precise orientation of loop II allows loop I, formed by residues Tyr-4 to Asn-16, to abut on top of the lid region of mAChE and be the second interaction point (Figure 1C). The tip of loop I, which contains the motif Thr–Thr–Thr–Ser–Arg–Ala that is also characteristic of fasciculins, inserts within a small crevice at the surface of mAChE and interacts with residues from loop b_3–$\alpha_{b3,2}$ and helices $\alpha_{b3,2}$ and $\alpha^3_{6,7}$, located 25 Å away from the gorge entrance (Figure 1C). Numerous polar interactions are found between the Fas2 Thr-8 side chain and the nitrogen backbone atoms of mAChE Val-73(71), Gln-279(272), and the Asp-283(276) side chains, between the Fas2 Thr-9 side chain and the mAChE Gln-279(272) side chain, and between the Fas2 Arg-11 side chain and the side chains of mAChE Glu-84(82) and Asn-87(85), conserved in all cholinesterase sequences (Figure 2B). Van der Waals contacts are observed between Fas2 His-6 and mAChE Thr-75(73), between Fas2 Thr-8 and mAChE Tyr-72(70), and between Fas2 Thr-9 and mAChE Tyr-70(68), Leu-92(90), and Val-282(275). The most critical residue in this interaction is Fas2 Ala-12, whose close packing with mAChE Pro-78(76), an amino acid protruding at the top of the gorge entrance, precludes substitution of a bulkier residue (Figure 2C).

The third interaction point between Fas2 and mAChE involves the side chains of residues Tyr-4 and Tyr-61, respectively located near and at the amino and carboxyl termini of Fas2, which establish van der Waals interactions with mAChE Tyr-77(75) and completely surround mAChE Pro-78(76) (Figure 2C). The close proximity of Fas2 Arg-37 also contributes to exclusion of Pro-78(76) from the solvent. These interactions substantially extend the area of the complex interface to a total of 1100 Å^2 buried to a 1.6 Å radius probe on each protein and encompasses 27% of the total surface area of Fas2 (Figure 3), two values in the highest range of general patterns for high affinity peptide–protein complexes (Janin and Chothia, 1990). Fas2 loop III, formed by residues Pro-42 to Lys-51, contributes weakly to the complex interface, as only residues Asn-47 and Leu-48, located at its tip, are in van der Waals interaction with mAChE through the His-287(280) side chain (Figure 3A); the other residues and the outside of β strand 5 are facing the solvent and are stabilized within the crystal by a symmetry-related mAChE molecule.

The Peripheral Anionic Site of mAChE

The key role played by the side chains of mAChE Tyr-72(70), Tyr-124(121), Trp-286(279), and Tyr-341(334), located at the rim of the gorge (Figure 2), in the binding of Fas2 closely matches previous site-directed mutagenesis data that defined these residues as belonging to the peripheral anionic site of the enzyme (Barak et al., 1994; Harel et al., 1992; Ordentlich et al., 1993; Radić et al., 1993; Shafferman et al., 1992) and, specifically, the binding site for Fas2 (Radić et al., 1994, 1995). This constellation of residues is unique to those AChEs that have high affinity for fasciculins. In contrast, the location of the conserved residue Asp-74(72) in the gorge entrance, relative to the other residues of the peripheral anionic site, is consistent with the limited influence of mutation of this residue on mAChE inhibition by Fas2 (Radić et al., 1994). Pro-78(76) and Gly-342(335) on mAChE also contribute to the fasciculin-binding site. Whether they should also be considered as part of the peripheral anionic site is, however, not certain. mAChE Pro-78(76) is conserved in all cholinesterase sequences and is positioned at the top of the lid rather than in the depression of the gorge entrance. The residual low affinity of fasciculins for insect and avian AChE as well as for BuChE could therefore arise from the interaction of Pro-78(76) with Fas2 residues Tyr-4, Ala-12, Arg-37, and Tyr-61, even in the absence of a contribution for loop II. Residue mAChE Gly-342(335), in close contact with Fas2 Lys-32, is highly conserved among the various cholinesterases, with the exception of insect AChE, where Asp is found. That substitution may partly explain the resistance of Drosophila AChE toward fasciculin inhibition.

Functional Residues of the Fasciculin Molecule

The predominance of basic amino acids on fasciculin, together with evidence for its interaction with an anionic site on AChE shared with cationic inhibitors of the enzyme, initially suggested a primary role for the positively charged side chains of fasciculin in its interaction with AChE. Recent studies, probing the functional role of the amino and guanidino groups of Fas2 through chemical modification, suggested that five positive residues, Arg-11, Lys-25, Arg-27, Lys-32, and Lys-51, comprise interacting sites of Fas2 (Cerveñansky et al., 1994, 1995). Initial site-directed mutagenesis data indicate that three to four positive residues, Arg-11, Arg-27, Lys-32, and perhaps Arg-24, contribute to the interaction sites of Fas2, whereas three others, Lys-25, Arg-28, and Lys-51, do not (P. M., unpublished data). These mutagenesis data correlate well with the Fas2–mAChE structure, including the role played by Arg-24 in stabilizing the side chain of Tyr-61 (the Fas2 Tyr-61 to mAChE Pro-78 interaction would weaken in the absence of Arg-24) (Figure 2C). Changes in the Fas2 structure may have occurred upon chemical modification of residues Lys-25 and Lys-51. In contrast, the reported absence of reactivity of Arg-24 to 1,2-cyclohexanedione is consistent with internal bonding within Fas2 rather than direct contact with mAChE.

Actually, only four out of the nine positively charged residues of Fas2 directly interact with mAChE: Arg-11, Arg-27, Lys-32, and Arg-37. The picomolar K_i values of the fasciculin–AChE complexes (Karlsson et al., 1984; Lin et al., 1987; Marchot et al., 1993; Radić et al., 1994; Eastman et al., 1995) arise in large part from the interactions of the hydrophobic residues located at the tips of loops I and II of Fas2. Nevertheless, six of the nine positively charged residues of fasciculin are located along loop II and, together with the isolated charge at the tip of loop I, play a major role in the approach and initial docking of the fasciculin to AChE (van den Born et al., 1995), consistent with the strong directional electrostatic field existing along the active center gorge axis (Ripoll et al., 1993).

Structural Adaptability and Specificity of the Fasciculin Molecule

Superimposition of the structure of Fas2 bound to mAChE with that of free Fas2 (Le Du et al., 1995) reveals that the tips of loops I and II are shifted by 2–2.5 Å within their respective mAChE-binding sites, resulting in a root mean square (rms) deviation of 0.77 Å for 61 Cα atoms (Figure 4A). Comparison of the crystal structures of Fas1 and Fas2, which differ by single mutation Tyr/Asn at position 47, revealed a large difference in the conformation of loop I, perhaps influenced by the detergent employed for crystallizing Fas2 (Le Du et al., 1992, 1995). It is noteworthy that mAChE Pro-78(76) plays exactly the same role as the side chain of Thr-9 in the structure of Fas1 in mimicking the detergent molecule that fills the hydrophobic pocket formed by Tyr-4, Arg-37, and Tyr-61 in the structure of Fas2 and allows free Fas2 to crystallize in a conformation resembling the bound state. In contrast, superimposition of free Fas1 with bound Fas2 reveals steric occlusion between loop I of Fas1 and the lid region of mAChE (Figure 4A), indicating that Fas1 binds to mAChE with a conformation of loop I different from that in the Fas1 crystal. The observations that crystallization yielded hexagonal Fas1–mAChE crystals belonging to the same space group and having the same cell dimensions as the Fas2–mAChE crystals (Marchot et al., submitted) and that Fas1 forms Fas2-type crystals in the presence of the detergent (Le

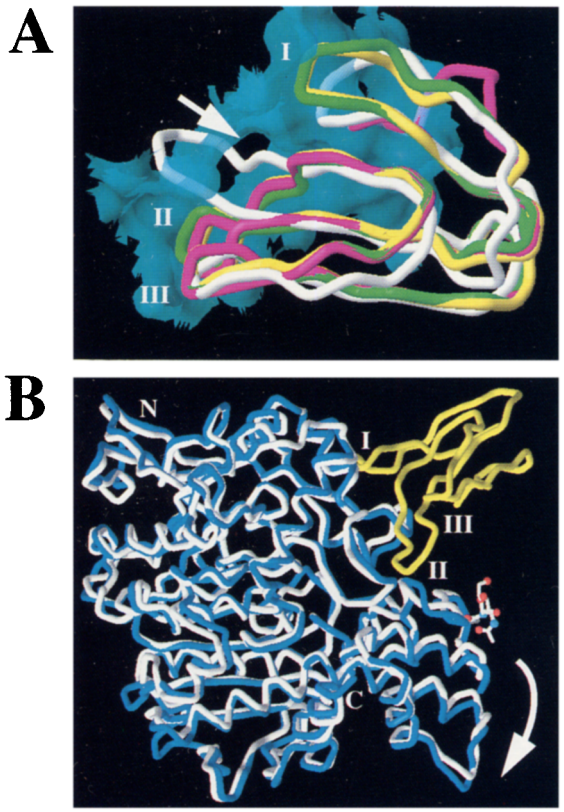

Figure 4. Comparison of Fas2 and mAChE with Their Respective Homologs

(A) Molecular surface of mAChE (blue) buried in the Fas2–mAChE complex, with the Cα traces of bound Fas2 (yellow), free Fas2 (green), free Fas1 (magenta), and toxin α (white). The toxin molecules are superimposed according to their Cα atoms. Steric occlusions of toxin α loops I and II and of Fas1 loop I with the mAChE interface are demonstrated by the surface transparency. The disulfide core and loop III conformations are conserved in all three-fingered toxins of known structure. The arrow indicates the mAChE active site gorge entrance.

(B) Superimposition of the mAChE monomer (blue) with a TcAChE monomer (white) according to their Cα atoms. The Fas2 molecule bound to mAChE is in yellow. The rigid body motion of residues Tyr-341(334) to Ser-399(392), at the bottom of the gorge entrance, is indicated by the curved arrow. The amino and carboxyl termini of the monomer are indicated by N and C, respectively. The GlcNAc moiety linked to Asn-350(343) is displayed in white with colored spheres.

Du et al., 1995) strongly support this hypothesis. These findings demonstrate the adaptability of the fasciculin molecule to its binding site on AChE, consistent with the general flexibility of the three-fingered toxins found by nuclear magnetic resonance (NMR) spectrometry (Brown and Wüthrich, 1992, and references therein).

Detailed structural information is available for the members of the three-fingered toxin family: α-neurotoxins, cardiotoxins, and muscarinic toxins (Endo and Tamiya, 1991; Rees and Bilwes, 1993; Segalas et al., 1995), and comparisons with fasciculins have already been made (Le Du et al., 1992, 1995: van den Born et al., 1995; Segalas et al., 1995). A cluster of Thr/Ser residues (loop I) exists in several short α-neurotoxins but is shifted by four to six residues and lacks an equivalent to Arg-11. Ala-12 exists only in fasciculins and in four of the short α-neurotoxins, all from Dendroaspis venoms. A unique short α-neurotoxin, toxin α from black mamba venom, possesses several of the fasciculin determinants for binding to AChE with Ser-8 (in place of Thr-8), Thr-9, Arg-11, and Ala-12 at the tip of its loop I, together with Tyr-4 in its disulfide core and, notably, a carboxy-terminal Tyr-61; it is, however, a fully potent α-neurotoxin (Strydom, 1972). Loop II of toxin α has none of the fasciculin determinants, except for the widely conserved Arg-37 and two Ile residues in place of Val-34 and Leu-35, and adopts the α-neurotoxin-typical conformation and orientation (Brown and Wüthrich, 1992). The presence of a Glu residue in toxin α in place of Gly-36 in Fas2 β strand 4 appears to be critical for dictating the backbone direction and, consequently, the bond angles of loop II (Figure 4A). Bond angles in loop II, governed by the above substitution and side chain compositions, distinguish the fasciculins from the α-neurotoxins and the muscarinic toxins (Le Du et al., 1992; Segalas et al., 1995). The specific shape of loop II allows perfect positioning of the key residue located at its tip: Met-33 in fasciculins, the conserved Arg residue in α-neurotoxins, and Lys-34 in the muscarinic agonist. In contrast, the conformation of loop III is highly conserved in all structures of three-fingered toxins. In fasciculins, loop III essentially appears to maintain a specific conformation of loop II through an extensive set of stabilizing interactions.

Comparison of mAChE and TcAChE Structures

Overall, a close structural similarity is observed between mAChE and TcAChE (Figure 4B). An rms deviation value of 0.84 Å for 509 Cα atoms is obtained when the two structures are superimposed. The largest difference is in the conformation of loop Glu-319(312) to Leu-324(317), resulting from the formation of a salt bridge between Asp-323(316) and Arg-223(216). Such a salt bridge cannot form in TcAChE, where Lys-316 is found. Within the active site, the shorter side chain of mAChE Pro-446, relative to Ile-439 in TcAChE, induces several rearrangements of the neighboring side chains: the Trp-439(432) side chain moves by 1.5 Å to maintain van der Waals contacts with the Pro-446 side chain, and the Phe-80(78) side chain slips in concert to keep interacting with Trp-439. The Tyr-337(330) side chain, which is hydrogen bonded to Tyr-441(334), adopts the conformation of the Phe-330 side chain in the edrophonium–TcAChE complex (Harel et al., 1993). Incidentally, this result confirms that no decamethonium was retained in the mAChE active site during purification (Marchot et al., submitted).

Some other substitutions are located at the binding interface that do not alter the backbone conformation but could modulate Fas2 interaction with the respective enzymes: mAChE Tyr-70 (Gln-68 in TcAChE), Thr-75 (Glu-73), Leu-76 (Gln-74), Tyr-77 (Phe-75), Leu-92 (Met-90), His-287 (Asn-280), and Glu-292 (Asp-285). The most critical of these appear to be the Leu-76→Gln substitution that brings to TcAChE a larger side chain that might interact differently with Arg-24, Val-34, and Arg-37 of Fas2 loop II, and the Thr-75→Glu and His-287→Asn substitutions

that cause charge differences that might change the interaction of loops II and III of Fas2. These substitutions could contribute to the ~100-fold lower affinity of Fas2 toward TcAChE compared to mAChE, mainly owing to a difference in the dissociation rate constants of the respective complexes (Z. Radić and G. Amitai, personal communication). Analysis of the Fas2–mAChE structure also revealed a GlcNAc moiety linked to mAChE at Asn-350 (Ser-343 in TcAChE), located ~14 Å away from the Fas2 Pro-30 anchoring point at the gorge entrance (Figures 2, 4, and 5).

Conformational Rearrangements in mAChE upon Binding of Fas2

The binding of Fas2 to mAChE does not induce a dramatic conformational change in the structure of complexed mAChE, when compared with TcAChE (Sussman et al., 1991). Several differences, however, are observed that might be related to conformational rearrangements of mAChE upon binding of Fas2. The first one is a rigid body motion of residues Tyr-341(334) to Ser-399(392), located at the bottom of the gorge entrance, with the largest deviation (up to 2.5 Å for residue Tyr-341) located closer to the top of the entrance (Figure 4B). However, the Asp-74(72) side chain moves in concert, and the hydrogen-bonding distance between the side chains of these two residues is conserved. The second difference between the two structures is a 1–1.5 Å deviation of the Asp-74(72) to Glu-84(82) region of mAChE, relative to its position in TcAChE. This displacement likely results from the tight fit of this region with the Pro-78(76)-binding area on Fas2. Finally, the surface cavity located near Glu-84(82) (and solvent molecule 27 in TcAChE) is enlarged owing to the translational movements of Tyr-341(334) and Asp-74(72), while the dimensions of the active site cavity near Trp-86(84) slightly increases owing to the internal movement of the Trp-439(432) side chain. In the Fas2–mAChE complex, the side chain of mAChE Thr-83(81) constitutes the unique barrier between the two cavities. A small gap between Fas2 loop I and mAChE keeps the surface cavity accessible to the solvent.

The tight packing of loop II of Fas2 at the gorge entrance seems to preclude the entrance of other molecules, even as small as water (Figure 2A). The structure of the Fas2–mAChE complex would suggest that the fasciculin mode of action is occlusion of substrate entry. Such a model, however, is not consistent with kinetic evidence showing that bound Fas2 and Fas3 fail to block completely subsequent organophosphate acylation and trifluoromethylacetophenone conjugation of the active center Ser (Marchot et al., 1993; Radić et al., 1995) and demonstrating the existence of detectable levels (0.1%–5%) of residual catalytic activity toward acetylthiocholine for the fasciculin–AChE complexes (Marchot et al., 1993; Marchot et al., submitted; Radić et al., 1994; 1995; Eastman et al., 1995). Fractional inhibition by fasciculin is even less for larger substrates of lower turnover rates such as p-nitrophenylacetate (Radić et al., 1995).

A similar enigma is encountered for the entry of active-site ligands in crystalline TcAChE, the gorge entrance of which is occluded by a symmetry-related molecule (Harel et al., 1993; Axelsen et al., 1994). Of the five ion pairs involved in the interaction of the gorge rim of TcAChE and the symmetry-related molecule, three residues (Glu-73 to Thr-75 in mAChE, Asp-276 to Asp-283 in mAChE, and Asp-285 to Glu-292 in mAChE) contribute to the Fas2–mAChE interaction and constitute ~20% of the buried interface area of the Fas2–mAChE complex. In addition, loop I of Fas2 resides on the lid of mAChE with Arg-11, extending to interact with mAChE Glu-84(82) and Asn-87(85), residues also conserved in TcAChE (Figure 2B). Both residues belong to the proposed back door region (Ripoll et al., 1993; Axelsen et al., 1994) and are immediate neighbors of Trp-86(84) that stabilizes the quaternary group of the substrate (Gilson et al., 1994). Thus, compatibility between the kinetic data and these new structural results requires either a second portal for both entry of substrates and exit of products in the complex or a conformational change in mAChE, not obvious in the crystal structure, opening a gap between the gorge wall and the bound fasciculin. A discrete shutter-like movement of the

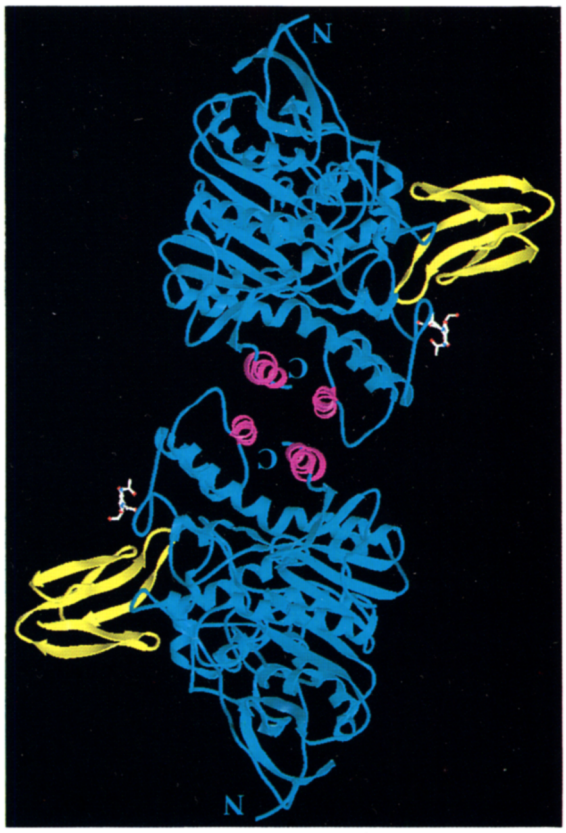

Figure 5. Dimeric Assembly of Monomeric mAChE

Ribbon diagram of the mAChE dimer (blue) with bound Fas2 (yellow) viewed down the crystallographic two-fold axis. The enzyme is devoid of an intersubunit disulfide-linking Cys and is monomeric in solution, but a dimer forms within the crystal. A four-helix bundle is formed by the tight packing of helices $\alpha^3_{7\,8}$ and α_{10} (magenta) from each monomer. The amino and carboxyl termini of each monomer are indicated by N and C, respectively. The two gorge entrances are at opposite faces. The GlcNAc moiety linked to Asn-350 (Ser-343 in TcAChE) is displayed in white with colored spheres.

side chain of Thr-83(81), located midway in the channel that we observe between Glu-84(82) and the mAChE active site, could occur simultaneously to the opening of a back door at Trp-86(84).

Dimeric Assembly of Monomeric mAChE

Recombinant mAChE was created by truncation of the carboxyl terminus through an early stop codon at position 549 (541 in TcAChE) and elimination of the intersubunit disulfide-linking Cys of recombinant form mAChE-H. The resulting product is monomeric and devoid of a carboxy-terminal hydrophobic segment (Marchot et al., submitted). Analysis of the Fas2–mAChE complex structure revealed that a homodimer assembles between two symmetry-related molecules in the crystal, arising from the tight packing of helices $\alpha^3_{7,8}$ and α_{10} from each mAChE monomer, which thus form the same four-helix bundle as previously observed for the disulfide-linked dimeric TcAChE (Sussman et al., 1991) (Figure 5). Since in dilute solution dimers were not detected by hydrodynamic and chromatographic analyses, oligomeric assembly of mAChE monomers through hydrophobic interactions outside of the Cys-containing carboxy-terminal segment may be facilitated by the high protein concentration or the high salt concentration in use for crystallization of the Fas2–mAChE complex (or both). However, hydrophobic interactions account for 77% of the 870 Å^2 interface area buried on each of the two mAChE monomers. Similarity of these values with general patterns observed in oligomeric proteins (Janin et al., 1988) suggests that the linking disulfide bridge is not the major determinant for dimer formation.

Significance and Implications

The crystal structure of the Fas2–mAChE complex offers a model for a three-fingered snake toxin in a complex with its specific receptor and reveals several features that are likely to be characteristic of the fasciculins, the α-neurotoxins, and the peptidic muscarinic agonists. First, the tips and exposed side surfaces of the loops govern the specificity of the toxin molecule. Additional segmental flexibility is accorded to these domains, and the φ and ψ bonds between the loop tip and base may serve essentially as joints to effect finger orientation. Second, an interdependence of the loop positions is also critical. In the case of fasciculin, loop I fits in a crevice near the lip of the gorge to maximize the surface area of contact of loop II at the gorge entry, therein serving to buttress the loop position.

Models of the muscarinic receptor, based on the bacteriorhodopsin structure (Henderson and Schertler, 1990), reveal that the seven transmembrane-spanning regions form the outer perimeter of a 20 Å cleft in which agonists and antagonists bind (Nordvall and Hacksell, 1993). Loop II of the muscarinic agonist toxin MTX2 contains the protruding Lys-34 at its tip (Segalas et al., 1995). Its position in the receptor cleft would enable it to interact with Asp-105, a residue found in transmembrane helix 3 and believed to contribute to the interaction sites for the quaternary moiety in ACh (Spalding et al., 1994). Insertion of the longer loop II into the muscarinic cleft could well arise from the appropriate apposition of loop I at a site near the cleft entrance (Segalas et al., 1995). Such a synergy between loops is also likely when the binding site encompasses an interface between two subunits, as for the α-neurotoxin-binding sites on the nicotinic receptor (Blount and Merlie, 1989; Bertrand and Changeux, 1995). Loop III in fasciculin may largely contribute to stabilizing the position in loop II, whereas in the α-neurotoxins it may interact more directly with the nicotinic receptor.

The structure of the fasciculin–AChE complex should enable the systematic design of mutations to ascertain the energetic contributions of the loops to the complex. Moreover, since loop II of fasciculin appears to occlude the entrance of the gorge of the enzyme, coupling of kinetic analyses, mutagenesis of individual residues comprising the interaction surface, and structural studies should prove informative for ascertaining the portal(s) of substrate entry into the complex.

Experimental Procedures

Crystallization and Data Collection

Details on expression and purification of recombinant mAChE and on preparation and crystallization of the Fas2–mAChE complex will be reported elsewhere (Marchot et al., submitted). The Fas2–mAChE complex generated two indistinguishable hexagonal crystal forms, A and B, obtained from identical crystallization conditions, both diffracting up to 2.8 Å. This resolution limit, however, could not be achieved because the crystals could not be flash cooled and were very sensitive to X-ray radiation. All data were therefore collected at 4°C. Form A crystals belong to space group $P6_522$ with cell dimensions a = b = 75.5 Å, c = 556.2 Å, giving a Vm value of 3.1 Å^3/Da (60% solvent; Matthews, 1968) for a single Fas2–mAChE complex in the asymmetric unit. A 3.2 Å resolution data set, which consisted of 62,214 observations for 14,488 unique reflections (85% complete; R_{sym} = 8.9%), was collected from four crystals with a crystal-to-detector distance of 862 mm (λ = 1 Å) and a 10.6° tilt or with a distance of 538 mm (λ = 1.5 Å) and a 12.4° tilt. In the 3.3–3.2 Å resolution range, the data set was 67% complete with an R_{sym} of 21%. Form B crystals also belong to space group $P6_522$ with cell dimensions a = b = 128.4 Å, c = 556.6 Å, giving the same Vm value as form A crystals for three Fas2–mAChE complexes in the asymmetric unit. A 3.5 Å resolution data set, which consisted of 92,846 observations for 33,798 unique reflections (87% complete; R_{sym} = 9.4%), was collected from four crystals with a distance of 757 mm (λ = 1.15 Å) and a 10° tilt. Data were collected at beam line X12C of the National Synchrotron Light Source with a MarResearch imaging plate detector and were processed with DENZO and SCALEPACK (Otwinowski, 1993).

Structure Solution and Refinement

Initial phases for the form A crystal data set were obtained by the molecular replacement method using the TcAChE model (PDB code, 1ACE) as a search model with the AMoRe program package (Navaza, 1994). The positioned mAChE (correlation = 51%; R factor = 41% in the 15 Å to 4 Å resolution range) was refined with X-PLOR (Brünger et al., 1987), which gave an R factor of 26% and a free R factor of 39% (5% of the reflections) in the 10 Å to 3.2 Å resolution range. The mAChE model was manually fitted, and a poly-Ala model corresponding to Fas2 was built into σ_A weighting electron density maps (Read, 1986) with the graphics program XFIT (McRee, 1992) and a modified version of TURBO-FRODO (Roussel and Cambillau, 1989; A. G. Inisan, A. Roussel, and C. Cambillau, personal communication). Subsequent refinements were performed alternating with model building until a 40 residue poly-Ala model, consisting of five segments, was obtained. Superimposition of Fas2 (PDB code, 1FSC) with the model revealed an orientation based on the position of the four disulfide bridges and the side chains of Tyr-27 and Tyr-61, together with the directions of loops I and II. This overlapped model was refined by rigid body motion in the 10 Å to 3.2 Å resolution range after removal of loops I and II, suspected of high flexibility, from Fas2. Successive

rounds of rebuilding and simulated annealing refinement allowed complete interpretation of both the Fas2 and mAChE structures. X-PLOR omit maps were used from the final model to check systematically every part of Fas2 and of the mAChE regions bound to Fas2: five and ten residues of the structures of Fas2 and mAChE, respectively, were deleted in each calculation, and simulated annealing was used to reduce model bias in the omit maps. The final model (model A, described herein) has a R factor of 18.4% for 13,823 reflections (all data) between 10 Å and 3.2 Å resolution and a free R factor of 29.4%. High temperature factors and weak electron density include mAChE residues Pro-492(485) to Pro-498. Fas2 residue Lys-51 and mAChE residues Arg-13(11), Arg-45(43), Arg-253(250), Arg-364(357), Arg-470(463), and Arg-493(486) are truncated to Cβ. The overall deviations from ideal geometry are 0.007 Å for bond distances and 1.5° for bond angles. The stereochemistry of the model was analyzed with PROCHECK (Laskowski et al., 1993), and 80% of the polypeptide backbone dihedral angles were found to lie in the most favored regions of the Ramachandran diagram. The coordinates of model A will be deposited with the Brookhaven Protein Data Bank.

The structure of form B was determined by molecular replacement with the AMoRe program using the refined model A. For three Fas2–mAChE complexes in the asymmetric unit, the correlation and R factors were 70% and 39%, respectively, in the 15 Å to 4 Å resolution range. Successive rounds of refitting were followed by refinement cycles. The final model (model B) has an R factor of 20.8% for 29,167 reflections (all data) in the 10 Å to 3.5 Å resolution range and a free R factor of 32.2%. The overall deviations from ideal geometry are 0.01 Å for bond distances and 1.7° for bond angles. Model B is essentially identical with model A and is not described herein.

Acknowledgments

Y. B. is a visiting scientist from the Laboratoire de Cristallisation et Cristallographie des Macromolécules Biologiques, Centre National de la Recherche Scientifique (CNRS), Institut Fédératif de Recherche Concertée, Marseille, France, and P. M. is a visiting scientist from the Laboratoire de Biochimie, CNRS, Univèrsité d'Aix-Marseille 2, Marseille, France. We are particularly indebted to Dr. Joel L. Sussman for encouragement and enthusiastic support of data collection at the National Synchrotron Light Source (NSLS), to Dr. Robert M. Sweet for access to the NSLS beam line X12C, and to Dr. John A. Tainer for liberal use of the facilities in his laboratory and for critical reading of the manuscript. We thank Dr. Zoran Radić for helpful discussions and details on unpublished kinetic data and Drs. Anne Gaël Inisan, Alain Roussel, and Christian Cambillau for the modified version of program TURBO-FRODO. This work was supported by United States Public Health Service GM18360 and Department of Army Medical Defense 17C grants to P. T. Drs. Michal Harel, Israel Silman, and Joel Sussman have independently developed a solution of the Fas2–TcAChE crystalline complex. A joint comparison of the coordinates of the two complexes should yield important information on the residue contributions to complex formation and conformation.

Received October 3, 1995; revised October 17, 1995.

References

Adem, A., Asblom, A., Johansson, G., Mbugua, P.M., and Karlsson, E. (1988). Toxins from the venom of the green mamba *Dendroaspis angusticeps* that inhibit the binding of quinuclidinylbenzylate to muscarinic acetylcholine receptors. Biochem. Biophys. Acta *968*, 340–345.

Axelsen, P.H., Harel, M., Silman, I., and Sussman, J.L. (1994). Structure and dynamics of the active site gorge of acetylcholinesterase: synergistic use of molecular dynamic simulation and X-ray crystallography. Protein Sci. *3*, 188–197.

Barak, D., Kronman, C., Ordentlich, A., Ariel, N., Bromberg, A., Marcus, D., Lazar, A., Velan, B., and Shafferman, A. (1994). Acetylcholinesterase peripheral anionic site degeneracy conferred by amino acid arrays sharing a common core. J. Biol. Chem. *264*, 6296–6305.

Bertrand, D., and Changeux, J.P. (1995). Nicotinic receptor: an allosteric protein specialized for intercellular communication. Neurosciences *7*, 75–90.

Blount, P., and Merlie, J. (1989). Molecular basis of the two nonequivalent ligand-binding sites of the muscle nicotinic acetylcholine receptor. Neuron *3*, 349–357.

Brown, L.R., and Wüthrich, K. (1992). Nuclear magnetic resonance solution structure of the α-neurotoxin from the black mamba (*Dendroaspis polylepis polylepis*). J. Mol. Biol. *227*, 1118–1135.

Brünger, A.T., Kuriyan, J., and Karplus, M. (1987). Crystallographic R-factor refinement by molecular dynamics. Science *235*, 458–460.

Cerveñansky, C., Dajas, F., Harvey, A.L., and Karlsson, E. (1991). Fasciculins, anticholinesterase toxins from mamba venoms: biochemistry and pharmacology. In Snake Toxins, A.L. Harvey, ed. (New York: Pergamon Press), pp. 303–321.

Cerveñansky, C., Engström, A., and Karlsson, E. (1994). Study of structure–activity relationship of fasciculin by acetylation of amino groups. Biochem. Biophys. Acta *1199*, 1–5.

Cerveñansky, C., Engström, A., and Karlsson, E. (1995). Role of arginine residues for the activity of fasciculin. Eur. J. Biochem. *229*, 270–275.

Changeux, J.P., Kasai, M., and Lee, C.Y. (1970). The use of a snake venom toxin to characterize the cholinergic receptor protein. Proc. Natl. Acad. Sci. USA *67*, 1241–1247.

Cygler, M., Schrag, J., Sussman, J.L., Harel, M., Silman, I., Gentry, M.K., and Doctor, B.P. (1993). Relationship between sequence conservation and three-dimensional structure in a large family of esterases, lipases, and related proteins. Protein Sci. *2*, 366–382.

Duran, R., Cerveñansky, C., Dajas, F., and Tipton, K.F. (1994). Fasciculin inhibition of acetylcholinesterase is prevented by chemical modification of the enzyme at a peripheral site. Biochem. Biophys. Acta *1201*, 381–388.

Eastman, J., Wilson, E.J., Cerveñansky, C., and Rosenberry, T.L. (1995). Fasciculin 2 binds to the peripheral site on acetylcholinesterase and inhibits substrate hydrolysis by slowing a step involving proton transfer during enzyme acylation. J. Biol. Chem. *270*, 19694–19701.

Endo, T., and Tamiya, N. (1991). Structure–function relationship of postsynaptic neurotoxins from snake venoms. In Snake Toxins, A.L. Harvey, ed. (New York: Pergamon Press), pp. 165–222.

Gilson, M.K., Straatsma, T.P., McCammon, J.A., Ripoll, D.R., Faerman, C.H., Axelsen, P.H., Silman, I., and Sussman, J.L. (1994). Open "back door" in a molecular dynamics simulation of acetylcholinesterase. Science *263*, 1276–1278.

Grochulski, P., Li, Y., Schrag, J.D., and Cygler, M. (1994). Two conformation states of *Candida rugosa* lipase. Protein Sci. *3*, 82–91.

Harel, M., Sussman, J.L., Krejci, E., Bon, S., Chanal, P., Massoulié, J., and Silman, I. (1992). Conversion of acetylcholinesterase to butyrylcholinesterase: modeling and mutagenesis. Proc. Natl. Acad. Sci. USA *89*, 10827–10831.

Harel, M., Schalk, I., Ehret-Sabatier, L., Bouet, F., Goeldner, M., Hirth, C., Axelsen, P.H., Silman, I., and Sussman, J.L. (1993). Quaternary ligand binding to aromatic residues in the active-site gorge of acetylcholinesterase. Proc. Natl. Acad. Sci. USA *90*, 9031–9035.

Henderson, R., and Schertler, G.F.X. (1990). The structure of bacteriorhodopsin and its relevance to the visual opsins and other seven-helix G-protein coupled receptors. Phil. Trans. R. Soc. (Lond.) B *326*, 379–389.

Janin, J., and Chothia, C. (1990). The structure of protein–protein recognition sites. J. Biol. Chem. *265*, 16027–16030.

Janin, J., Miller, S., and Chothia, C.H. (1988). Surface, subunit interfaces and interior of oligomeric proteins. J. Mol. Biol. *204*, 155–164.

Karlsson, E., Mbugua, P.M., and Rodriguez-Ithurralde, D. (1984). Fasciculins, anticholinesterase toxins from the venom of the green mamba *Dendroaspis angusticeps*. J. Physiol. *79*, 232–240.

Laskowski, R.A., MacArthur, M.W., Moss, D.S., and Thornton, J.M. (1993). PROCHEK: a program to check the stereochemical quality of protein structures. J. Appl. Cryst. *26*, 283–291.

Le Du, M.H., Marchot, P., Bougis, P.E., and Fontecilla-Camps, J.C. (1992). 1.9 Å resolution structure of fasciculin 1, an anti-cholinesterase toxin from green mamba snake venom. J. Biol. Chem. *267*, 22122–22130.

Le Du, M.H., Housset, D., Marchot, P., Bougis, P.E., Navaza, J., and Fontecilla-Camps, J.C. (1995). Crystal structure of fasciculin 2 from mamba snake venom: evidence for unusual loop flexibility. Acta Crystallogr., in press.

Lin, W.W., Lee, C.Y., Carlsson, F.H.H., and Joubert, F.J. (1987). Anticholinesterase activity of angusticeps-type toxins and protease inhibitor homologues from mamba venoms. Asia Pac. J. Pharmacol. *2*, 79–85.

Marchot, P., Khélif, A., Ji, Y.H., Mansuelle, P., and Bougis, P.E. (1993). Binding of ^{125}I-fasciculin to rat brain acetylcholinesterase: the complex still binds diisopropyl fluorophosphate. J. Biol. Chem. *268*, 12458–12467.

Massoulié, J., Pezzementi, L., Bon, S., Krejci, E., and Vallette, F.M. (1993). Molecular and cellular biology of the cholinesterases. Prog. Neurobiol. *41*, 31–91.

Matthews, B.W. (1968). Solvent content of protein crystals. J. Mol. Biol. *33*, 491–497.

McRee, D.E. (1992). A visual protein crystallographic software system for X11/Xview. J. Mol. Graph. *10*, 44–47.

Navaza, J. (1994). AMoRe: an automated package for molecular replacement. Acta Crystallogr. *A50*, 157–163.

Nordvall, G., and Hacksell, U. (1993). Binding-site modeling of the muscarinic m1 receptor: a combination of homology-based and direct approaches. J. Med. Chem. *36*, 967–976.

Ordentlich, A., Barak, D., Kronman, C., Flashner, Y., Leitner, M., Segall, Y., Ariel, N., Cohen, S., Velan, B., and Shafferman, A. (1993). Dissection of the human acetylcholinesterase active center determinants of substrate specificity. J. Biol. Chem. *268*, 17083–17095.

Otwinowski, Z. (1993). Oscillation data reduction program. In Proceedings of the CCP4 Study Weekend, L. Sawyer, N. Isaacs, and S. Burley, eds. (Warrington, England: Science and Engineering Research Council/Daresbury Laboratory), pp. 56–62.

Rachinsky, T.L., Camp, S., Li, Y., Ekström, J., Newton, M., and Taylor, P. (1990). Molecular cloning of mouse acetylcholinesterase: tissue distribution of alternatively spliced mRNA species. Neuron *5*, 317–327.

Radić, Z., Pickering, N.A., Vellom, D.C., Camp, S., and Taylor, P. (1993). Three distinct domains in the cholinesterase molecule confer selectivity for acetyl- and butyrylcholinesterase inhibitors. Biochemistry *32*, 12074–12084.

Radić, Z., Duran, R., Vellom, D.C., Li, Y., Cerveñansky, C., and Taylor, P. (1994). Site of fasciculin interaction with acetylcholinesterase. J. Biol. Chem. *269*, 11233–11239.

Radić, Z., Quinn, D.M., Vellom, D.C., Camp, S., and Taylor, P. (1995). Allosteric control of acetylcholinesterase catalysis by fasciculin. J. Biol. Chem. *270*, 20391–20399.

Read, R.J. (1986). Improved Fourier coefficients for maps using phase from partial structure with errors. Acta Crystallogr. *A42*, 140–149.

Rees, B., and Bilwes, A. (1993). Three-dimensional structure of neurotoxins and cardiotoxins. Chem. Res. Toxicol. *6*, 385–406.

Ripoll, D.R., Faerman, C.H., Axelsen, P.H., Silman, I., and Sussman, J.L. (1993). An electrostatic mechanism for substrate guidance down the aromatic gorge of acetylcholinesterase. Proc. Natl. Acad. Sci. USA *90*, 5128–5132.

Roussel, A., and Cambillau, C. (1989). TURBO-FRODO. In Silicon Graphics Geometry Partners Directory, Silicon Graphics Committee, eds. (Mountain View, California: Silicon Graphics), pp 77–78.

Segalas, I., Roumestand, C., Zinn-Justin, S., Gilquin, B., Ménez, R., Ménez, A., and Toma, F. (1995). Solution structure of a green mamba toxin that activates muscarinic acetylcholine receptors, as studied by nuclear magnetic resonance and molecular modeling. Biochemistry *34*, 1248–1260.

Shafferman, A., Velan, B., Ordentlich, A., Kronman, C., Grosfeld, H., Leitner, M., Flashner, Y., Cohen, S., Barak, D., and Ariel, N. (1992). Substrate inhibition of acetylcholinesterase: residues affecting signal transduction from the surface to the catalytic center. EMBO J. *11*, 3561–3568.

Shafferman, A., Ordentlich, A., Barak, D., Kronman, C., Ber, R., Bino, T., Ariel, N., Osman, R., and Velan, B. (1994). Electrostatic attraction by surface charge does not contribute to the catalytic efficiency of acetylcholinesterase. EMBO J. *13*, 3448–3455.

Spalding, T.A., Birdsall, N.J.M., Curtis, C.A.M., and Hulme, E.C. (1994). Acetylcholine mustard labels the binding site aspartate in muscarinic acetylcholine receptors. J. Biol. Chem. *269*, 4092–4097.

Strydom, D.J. (1972). Snake venom toxins: the amino acid sequences of two toxins from *Dendroaspis polylepis polylepis* (black mamba) venom. J. Biol. Chem. *247*, 4029–4042.

Sussman, J.L., Harel, M., Frolow, F., Oefner, C., Goldman, A., Toker, L., and Silman, I. (1991). Atomic structure of acetylcholinesterase from *Torpedo californica*: a prototypic acetylcholine-binding protein. Science *253*, 872–879.

Tan, R.C., Truong, T.N., McCammon, J.A., and Sussman, J.L. (1993). Acetylcholinesterase: electrostatic steering increases the rate of ligand binding. Biochemistry *32*, 401–403.

Taylor, P., and Radić, Z. (1994). The cholinesterases: from genes to proteins. Annu. Rev. Pharmacol. Toxicol. *34*, 281–320.

van den Born, H.K.L., Radić, Z., Marchot, P., Taylor, P., and Tsigelny, I. (1995). Theoretical analysis of the structure of the peptide fasciculin and its docking to acetylcholinesterase. Protein Sci. *4*, 703–715.